Behavior and Surface Energies of Polybenzoxazines formed by Polymerization with Argon, Oxygen, and Hydrogen Plasmas

JEM-KUN CHEN,[1] I-KUAN LIN,[3] FU-HSIANG KO,[2] CHIH-FENG HUANG,[1] KUO-SHEN CHEN,[3] CHIA-HAO CHAN,[1] FENG-CHIH CHANG[1]

[1]National Chiao Tung University, Department of Applied Chemistry, Hsinchu, Taiwan

[2]National Nano Device Laboratories, 1001-1, Ta-Hsueh Road, Hsinchu 30050, Taiwan

[3]National Cheng Kung University, Department of Mechanical Engineering, Tainan 70101, Taiwan

ABSTRACT: Polybenzoxazine (PBZZ) thin films can be fabricated by the plasma-polymerization technique with, as the energy source, plasmas of argon, oxygen, or hydrogen atoms and ions. When benzoxazine (BZZ) films are polymerized through the use of high-energy argon atoms, electronegative oxygen atoms, or excited hydrogen atoms, the PBZZ films that form possess different properties and morphologies in their surfaces. High-energy argon atoms provide a thermodynamic factor to initiate the ring-opening polymerization of BZZ and result in the polymer surface having a grid-like structure. The ring-opening polymerization of the BZZ film that is initiated by cationic species such as oxygen atoms in plasma, is propagated around nodule structures to form the PBZZ. The excited hydrogen atom plasma initiates both polymerization and decomposition reactions simultaneously in the BZZ film and results in the formation of a porous structure on the PBZZ surface. We evaluated the surface energies of the PBZZ films polymerized by the action of these three plasmas by measuring the contact angles of diiodomethane and water droplets. The surface roughness of the films range from 0.5 to 26 nm, depending on the type of carrier gas and the plasma-polymerization time. By estimating changes in thickness, we found that the PBZZ film synthesized by the oxygen plasma-polymerization process undergoes the slowest rate of etching in CF_4 plasma. © 2004 Wiley Periodicals, Inc. J Polym Sci Part B: Polym Phys 42: 4063–4074, 2004
Keywords: polybenzoxazine; plasma treatment; surface free energy
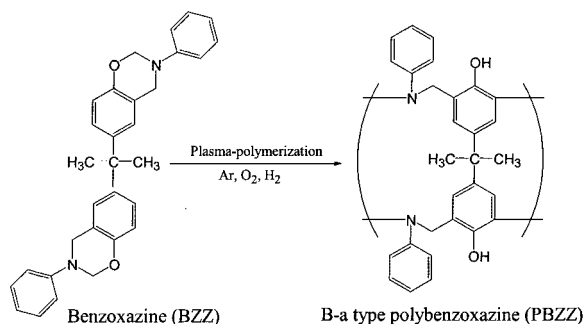
INTRODUCTION

Plasma-polymerization, which can be performed by conventional means, such as photochemical or free-radical initiation, is an important and unique

Correspondence to: F.-C. Chang (E-mail: changfc@mail. nctu.edu.tw)

technique for developing surface-specific materials. When a polymeric material is treated with plasma, only the surface properties of the substrate are changed; the bulk properties remain the same.[1–5] The treatment of polymeric materials with plasma causes surface modifications that affect the chemical composition as well as the surface topography. One example is the synthesis of composite materials consisting of both hydrophilic and hydrophobic components.[6]

4064 CHEN ET AL.

Scheme 1

Treatment with the so-called carrier gas can initiate polymerization, with the mode of the reaction depending on the types of gases. Argon atoms can be used as carriers of the excitation energy in plasma, that is, as a medium for energy transference. Argon plasma has been observed to modify polymer surfaces, such as acrylamides,[7] vinyl polymers,[8] and surface-initiated polymerization by means of self-assembled monolayers.[9,10] Because molecular oxygen is an electronegative gas, it forms stable negative ions. Oxygen plasma-induced reactions have become important processes in polymer surface modification. The process of oxygen plasma treatment has certain advantages over other surface-modifying techniques such as grafting reactions[11] or wet chemical treatments.[12] Remote hydrogen plasma treatment is a relatively new and extremely useful technique that offers well-controlled deposition conditions and provides films that are free of the damage that is usually observed when various chemical vapor deposition (CVD) methods are used in the fabrication of inorganic films.[13,14] Therefore, the use of different plasma carrier gases can result in different kinetics, structure, composition, and surface morphology of polymer films.

The structure of polybenzoxazine (PBZZ) is similar to that of phenolic resin; it is formed through a thermal self-curing process: a hetero-

cyclic ring-opening reaction that requires no catalyst and releases no condensation byproducts.[15] PBZZ resins possess several outstanding proper-

(a)

(b)

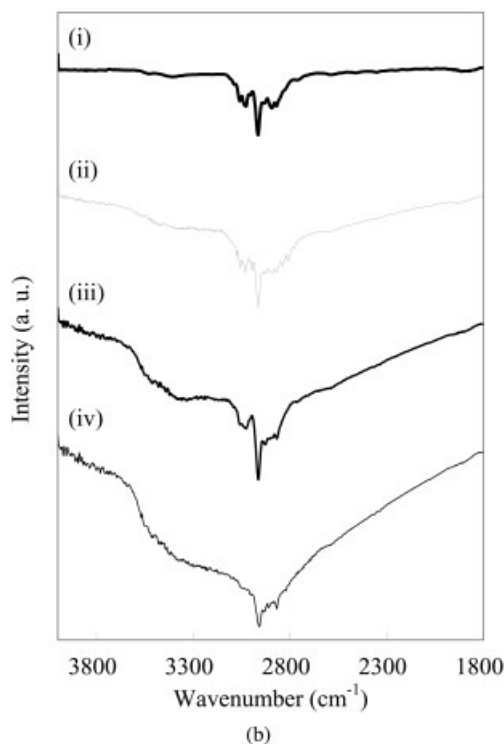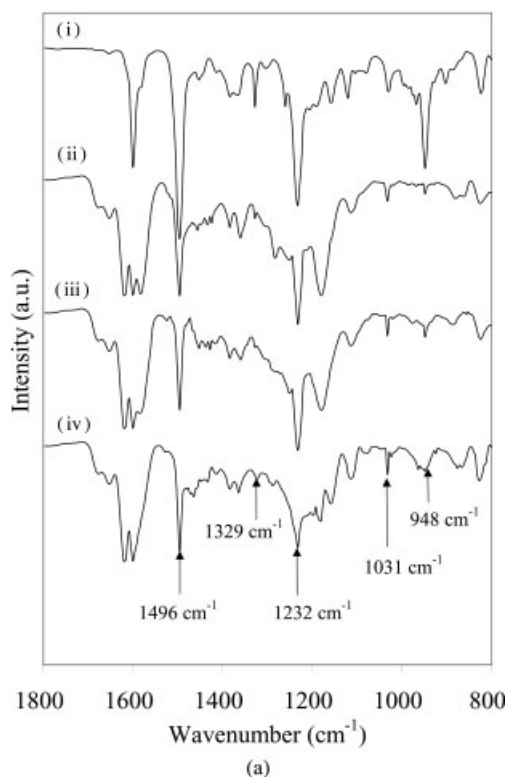**Figure 2.** (*Continued*)

Figure 1. (a) FTIR spectra of (i) BZZ film and PBZZ films treated by (ii) argon, (iii) oxygen, and (iv) hydrogen plasma for 90 s. The characteristic absorption is near 948, 1031, 1232, 1329, and 1496 cm^{-1}. (b) FTIR spectra of (i) BZZ film and PBZZ films treated by (ii) hydrogen, (iii) argon, and (iv) oxygen plasma for 90 s. The characteristic absorption is between 2500 and 3600 cm^{-1}.
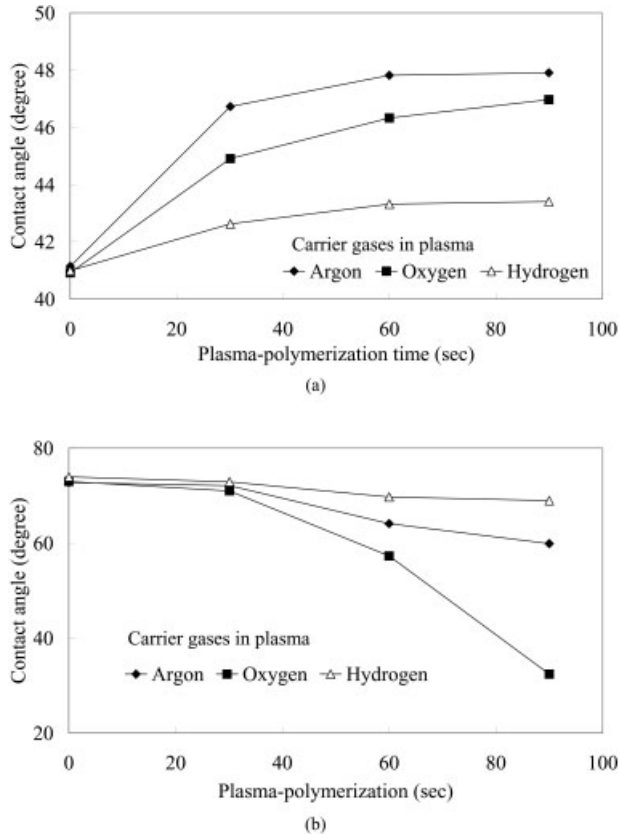
(a)

(b)

Figure 2. Contact angle of (a) diiodomethane and (b) water of argon, oxygen, and hydrogen plasma treated BZZ film with the increase of plasma treatment time.

ties, such as near-zero shrinkage after curing, high thermal stability, and low water absorption[16]; in addition, PBZZ has a high glass-transition temperature (T_g) even thought it has a relatively low crosslinking density.[17] In this study, we focused on the use of argon, oxygen, and hydrogen plasmas as energy sources for polymerizing benzoxazine (BZZ) films and on inducing reactions on the surfaces of the PBZZ films. We place special emphasis on the morphologies
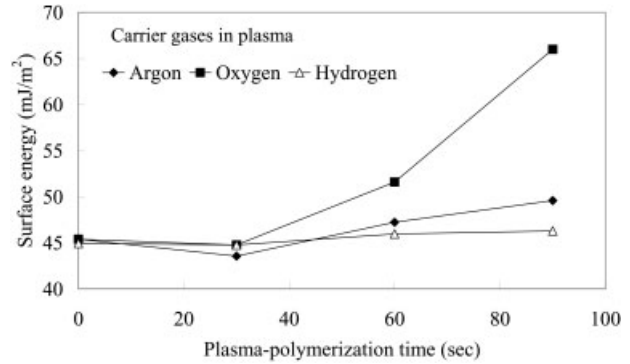

Figure 3. Surface free energies of argon, oxygen, and hydrogen plasma treated BZZ film with the increase of plasma treated time.

of the BZZ films that were polymerized under the influence of argon atoms with high energy, electronegative oxygen atoms, and excited hydrogen atoms. In addition, we evaluated the surface energies of the PBZZ films treated with argon, oxygen, and hydrogen plasma by measurement of their contact angles. Our estimation of the etching rates by measuring changes in thickness reveals the stability of the PBZZ films polymerized by the collision of atoms in plasma.

EXPERIMENTAL

Materials and Processing

We synthesized BZZ according to Ning and Ishida's procedure.[18] BZZ contains an oxazine ring that forms a phenolic structure on polymerization, as depicted in Scheme 1.

Plasma Treatment of BZZ Films

To form a BZZ film, we first primed a silicon wafer with hexamethyldisilazane (Merck, Darmstadt,

Table 1. The Surface Energy of the Dispersive and Polar Components Calculated from the Contact Angle of Diiodomethane and Water

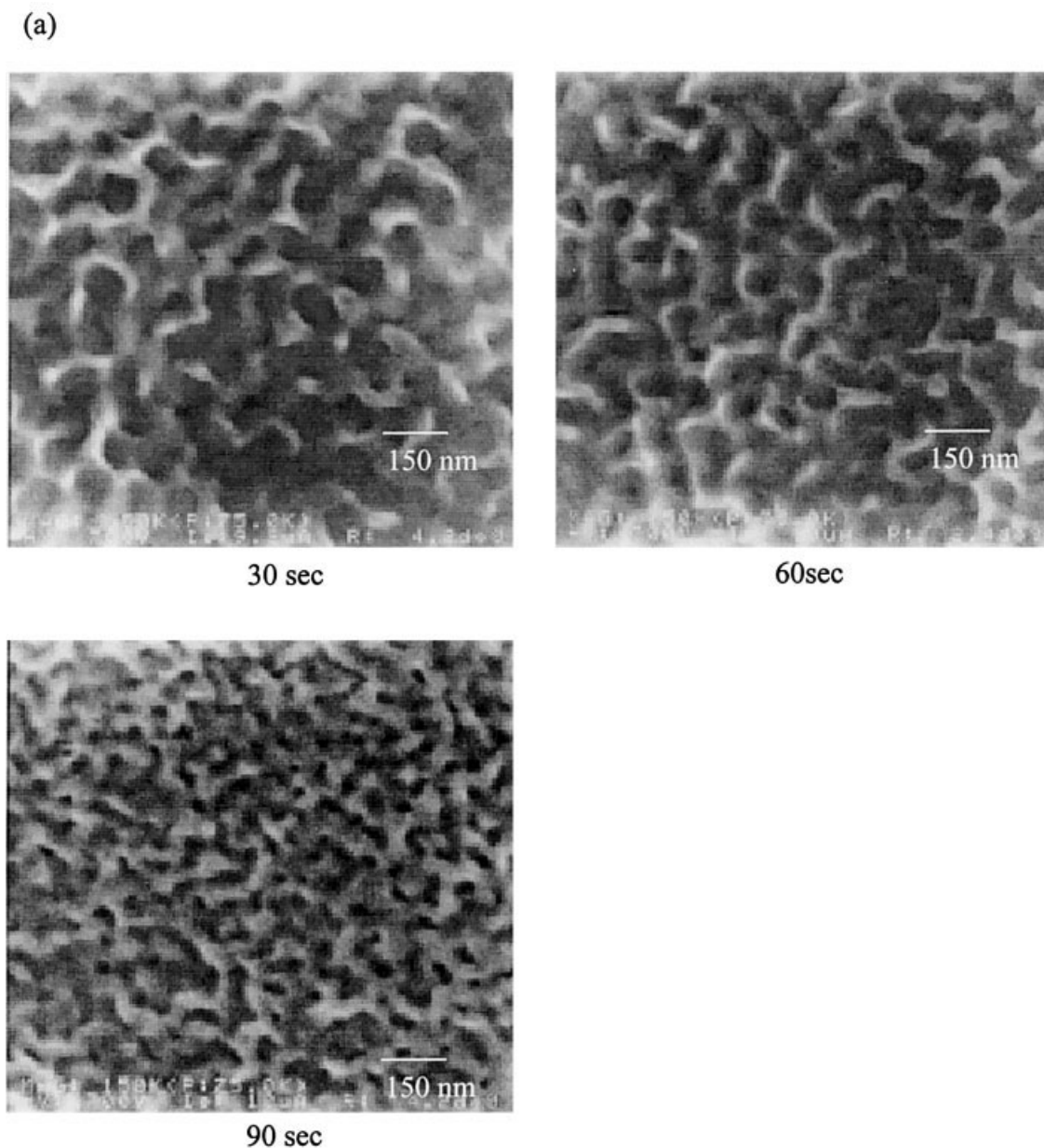| Reaction time (s)	Dispersive component (mJ/m^2)			Polar component (mJ/m^2)		
	Argon	Oxygen	Hydrogen	Argon	Oxygen	Hydrogen
0	22.2	22.3	22.5	12.5	12.3	11.6
30	21.5	21.4	22.0	9.8	4.0	4.8
60	20.5	21.0	21.4	20.7	24.1	8.4
90	19.9	20.4	21.2	23.7	42.1	15.0

(a)

30 sec

60sec

90 sec

Figure 4. Scanning electron micrographs of PBZZ film that were treated (a) with argon, (b) oxygen, and (c) hydrogen plasma for the series time.

Germany). BZZ was then spun onto the silicon wafer—the thickness of the BZZ film was 3575 nm at a spin rate of 1000 rpm (0.5 min duration)—and subjected to soft baking (110 °C, 30 s). Plasma-polymerization was conducted in a plasma-enhanced chemical vapor deposition (PECVD) chamber (STS, UK) operating at a frequency of 380 kHz and a power output of 250 W. Fourier transform infrared (FTIR) spectroscopy (Bio-Rad, Model FTS-40, MA, USA) was used to characterize the structural change that BZZ un-

dergoes during the plasma-polymerization process. The surface roughness and microscale profile were measured with an atomic force microscope (AFM, Digital Instruments, DI-5000, USA). The morphology was evaluated with an inline scanning electron microscope (SEM; Hitachi S-6280H, Tokyo, Japan).

Contact Angles

We examined the surface properties of the BZZ films by measuring contact angles. The advancing
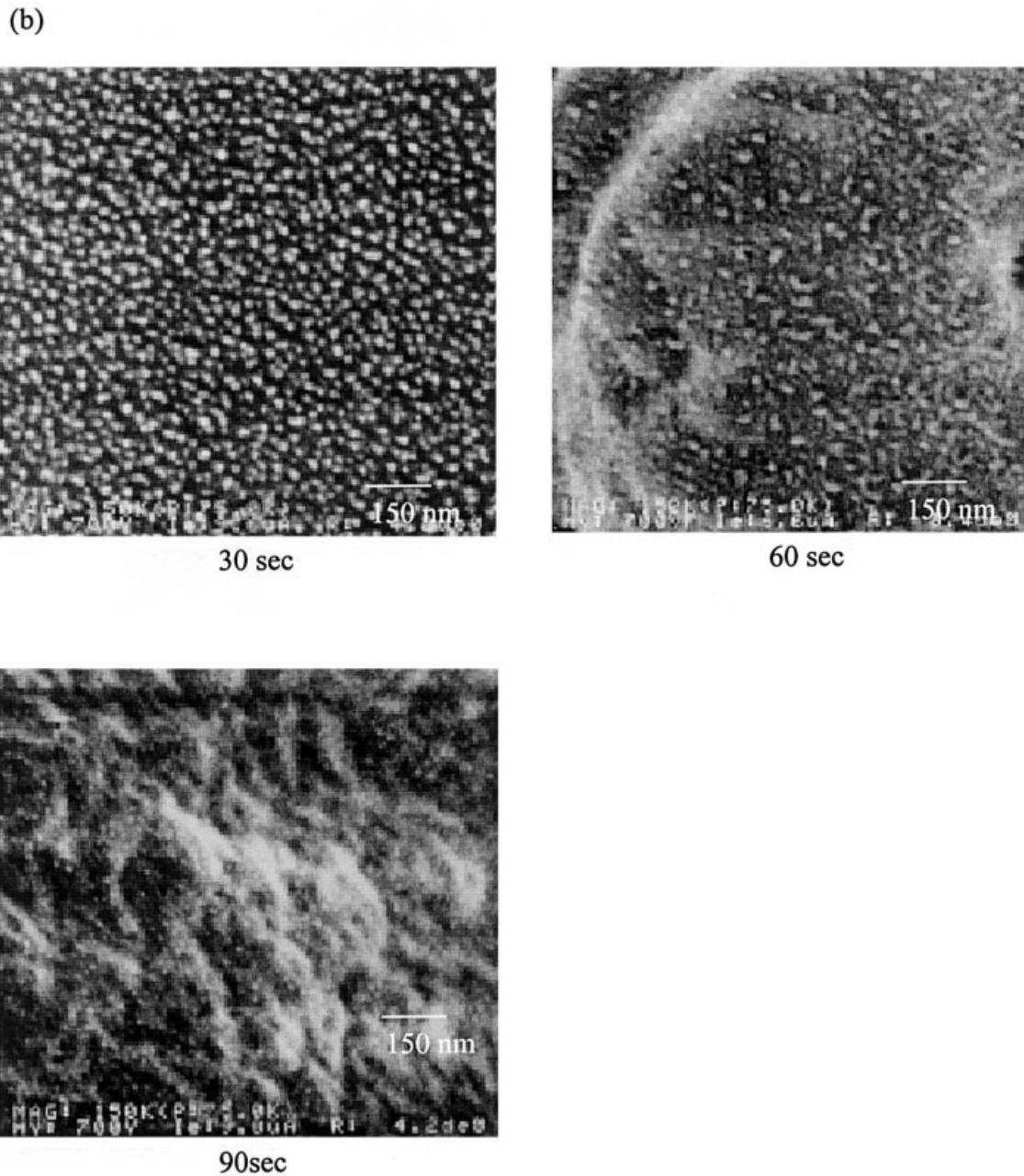
(b)

30 sec

60 sec

90sec

Figure 4.   *(Continued from the previous page)*

contact angles of water and diiodomethane were measured by increasing the water drop volume with a contact angle goniometer (GH-100, Krüss, Germany). With regard to the known contact angles of water and diiodomethane, we calculated the surface energies of the PBZZ films with the following equations[19,20]:

$$\gamma = \gamma^d + \gamma^p$$

$$(1+\cos\theta_1)\gamma_1 = 2(\gamma_s^d\gamma_1^d)^{1/2} + 2(\gamma_s^p\gamma_1^p)^{1/2} \qquad (1)$$

$$(1+\cos\theta_2)\gamma_2 = 2(\gamma_s^d\gamma_2^d)^{1/2} + 2(\gamma_s^p\gamma_2^p)^{1/2} \qquad (2)$$

where γ is the surface free energy, γ^d is the dispersive term of the surface free energy, γ^p is the polar term of the surface free energy, γ_s is the surface free energy of the membrane, θ_1 is the contact angle of water, θ_2 is the contact angle of diiodomethane, γ_1 is the surface free energy of water, and γ_2 is the surface free energy of diiodomethane.

(c)

30 sec

60 sec
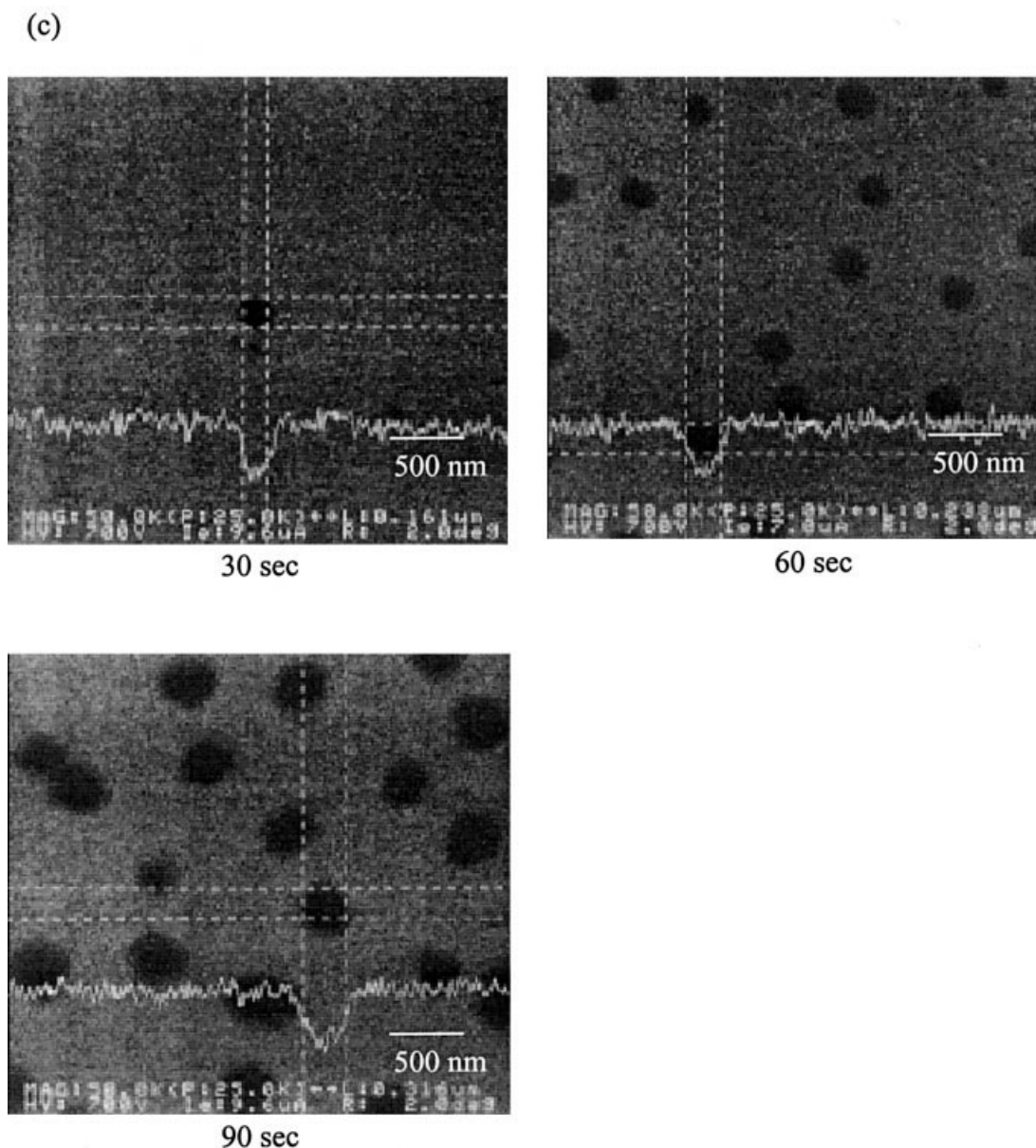

90 sec

Figure 4. *(Continued from the previous page)*

RESULTS AND DISCUSSION

Reaction Mechanism Analysis

Figure 1 provides the FTIR spectra of the PBZZ film obtained after plasma treatment for 90 s with hydrogen, oxygen, and argon gases, respectively. The characteristic absorptions of BZZ appear at 1232 (asymmetric stretching of the C—O—C unit), 1329 (CH_2 wagging), and at 948 and 1496 cm^{-1} (vibrations of the trisubstituted benzene ring). After plasma curing for 90 s with the various gases, the characteristic absorption band of the trisubstituted benzene ring at 948 cm^{-1} has almost completely disappeared, whereas that at 1496 cm^{-1} has reduced; the band at 1329 cm^{-1}, because of CH_2 wagging, also has decreased in intensity.[21] The absorption bands at 1031 and 1232 cm^{-1} that we assign to the symmetric and asymmetric stretchings of the C—O—C unit, have not disappeared completely.[22] Characteristic O—H bands appear between 3600 and 2500 cm^{-1} for the B-a-type PBZZ films treated with the argon, oxygen, and hydrogen plasma-polymerization conditions. The PBZZ film that we
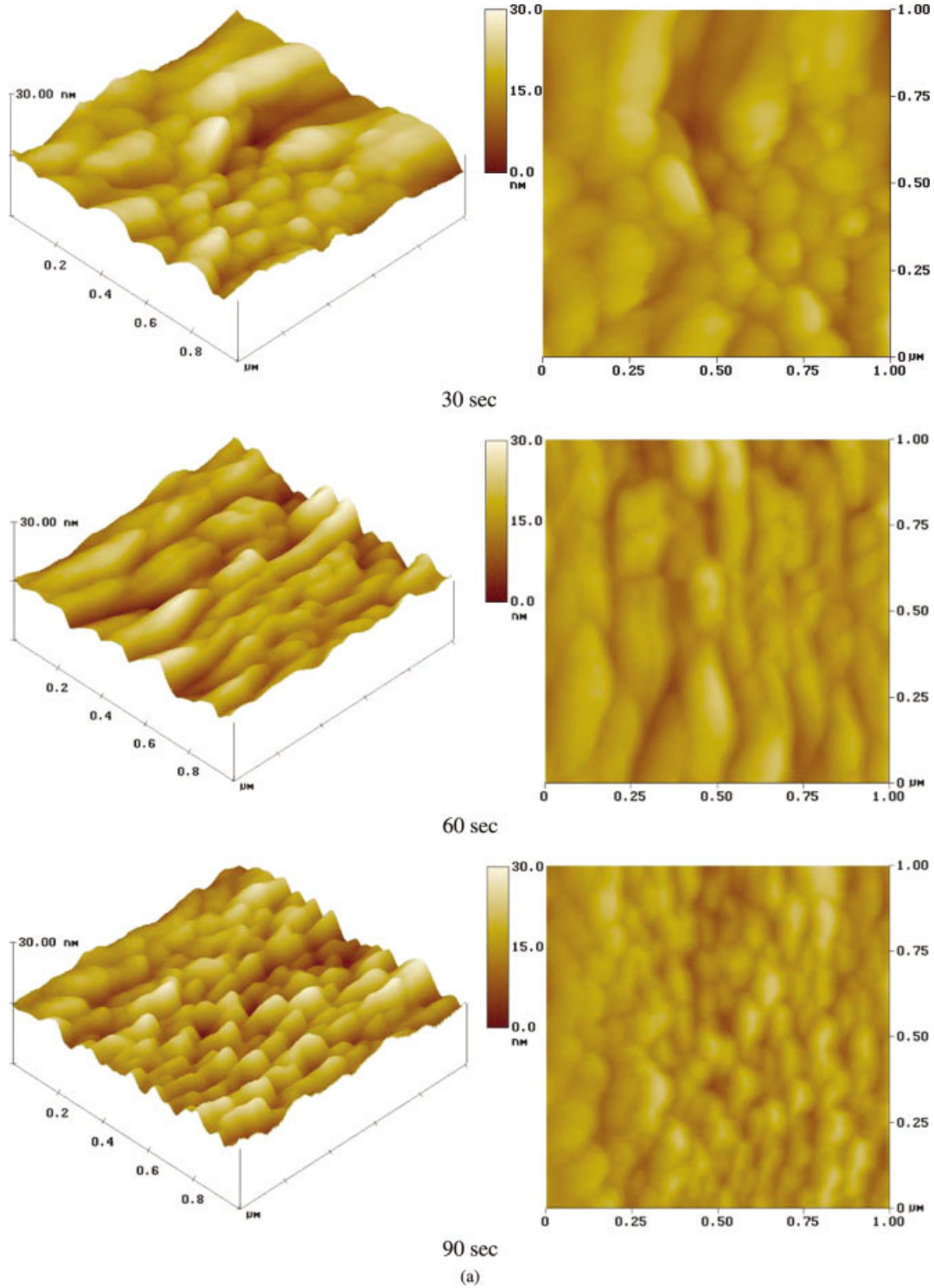
Figure 5. AFM images (1 μm $\times$ 1 μm) of the PBZZ surface modified with (a) argon, (b) oxygen, and (c) hydrogen plasma for the series reaction time.
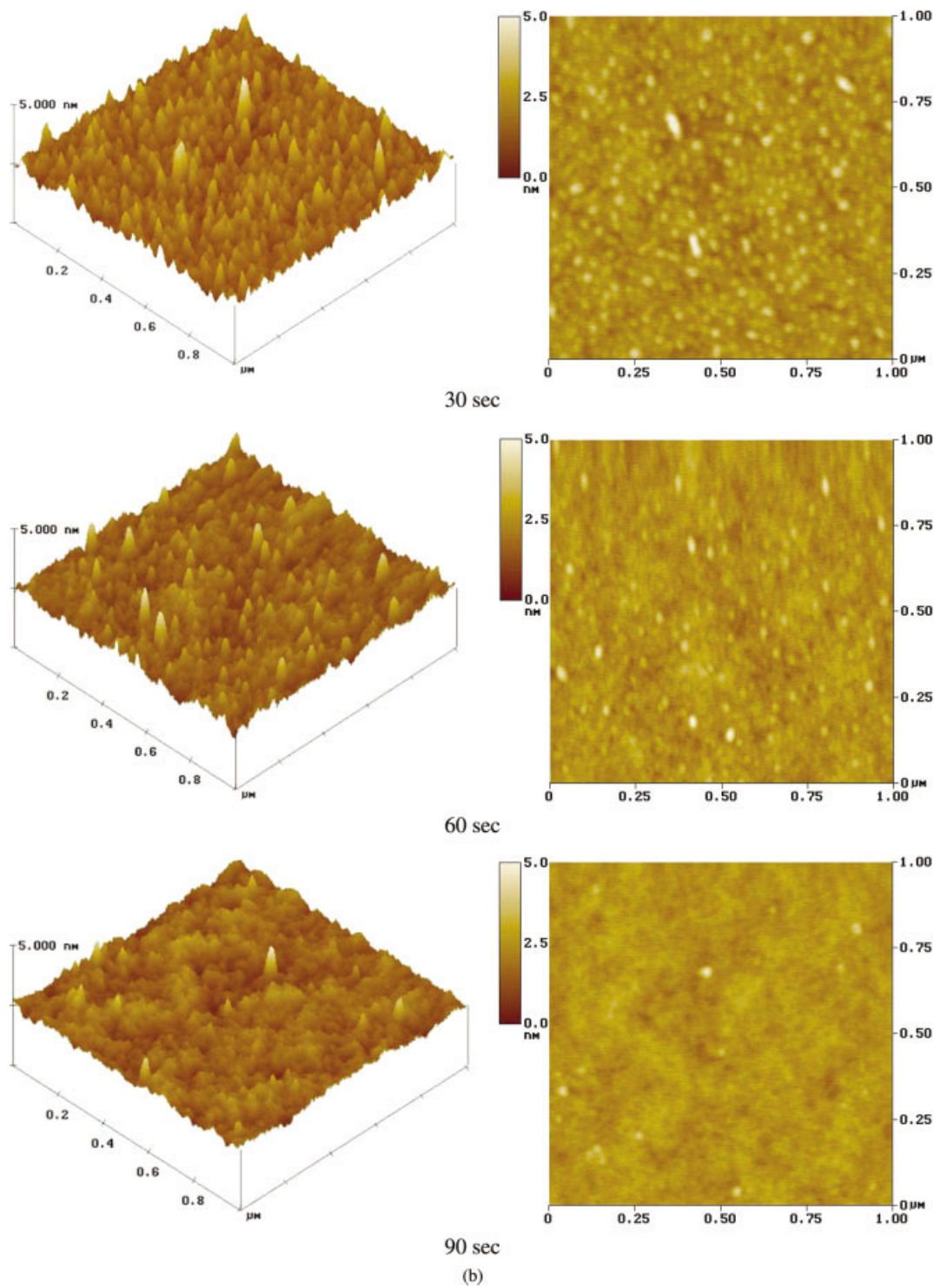
30 sec

60 sec

90 sec

(b)

Figure 5. *(Continued from the previous page)*
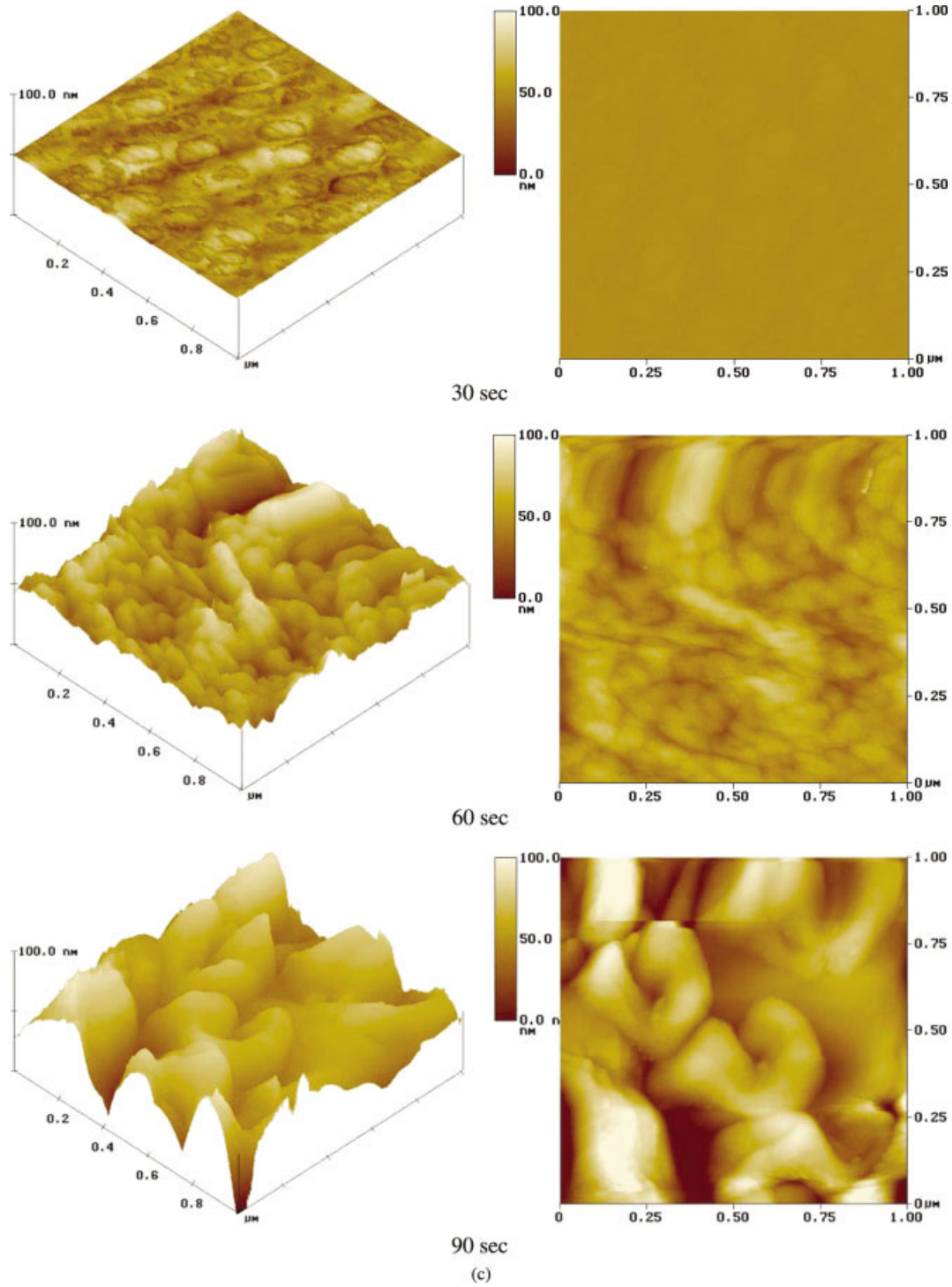
30 sec

60 sec

90 sec

(c)

Figure 5. *(Continued from the previous page)*

treated with the oxygen plasma exhibits the strongest broad peak for these hydroxyl groups, suggesting that strong hydrogen bonds form as a result of the hydrophilic effect caused by the oxygen plasma. The PBZZ film polymerized by the action of excited hydrogen atoms results in a weak hydroxyl peak because the excited hydrogen atoms in the plasma react with the hydroxyl groups of the phenolic units of PBZZ.

Contact Angles and Surface Free Energies

Figures 2(a and b) show the contact angles of diiodomethane and water droplets on the BZZ films produced by the argon, oxygen, and hydrogen plasma-induced polymerization as a function of the reaction times. The contact angle of the diiodomethane droplet increases when increasing the plasma-polymerization time [Fig. 2(a)]. This result suggests that the dispersive term of the surface free energy of the PBZZ film is lower than that of the BZZ because the polymerization is an exothermic reaction and, thus, it decreases the dispersive energy term. Figure 2(b) illustrates that the contact angle of the water droplet decreases when the plasma-polymerization time is increased because hydrophilic phenolic groups are formed on the surface of the hydrophobic BZZ during the plasma-polymerization process.[23,24] In addition, the polar term of the surface energy is increased on increasing the phenolic group content arising from the polymerization of BZZ. The capability of the carrier gases to form hydrophilic phenolic groups increases in the following order: oxygen > argon > hydrogen. Table 1 lists the surface energies based on the dispersive and po-
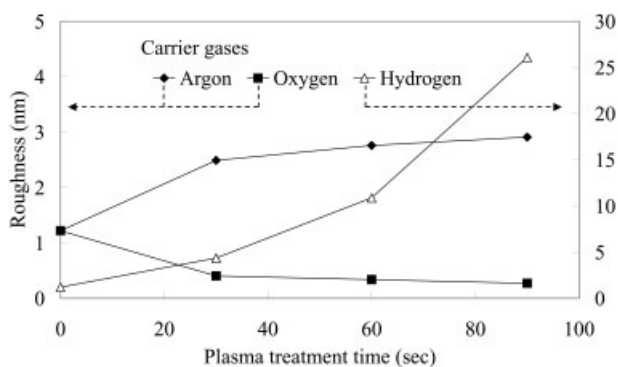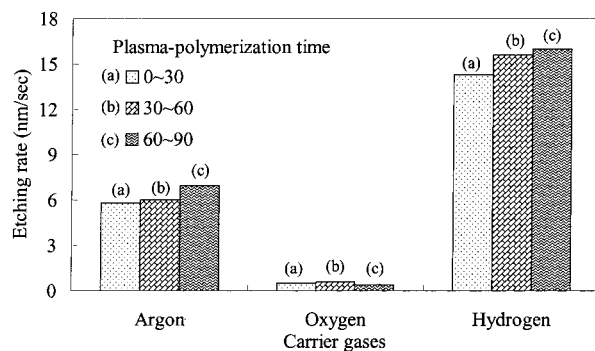

Figure 7. The etching rate of the PBZZ films as the argon, oxygen, and plasma were treated for 90 s in CF_4 plasma.

lar components calculated from the contact angles for the diiodomethane and water droplets. Figure 3 illustrates the total surface free energies of the argon, oxygen, and hydrogen plasma-treated BZZ films as a function of time. The surface free energies decrease slightly during the initial 30 s of the plasma-polymerization process as a result of the exothermic polymerization reaction. After 30 s, the surface energies increase with increasing plasma-polymerization time up to 60 s, during which time the surface energy depends mainly on the polar component rather than the dispersive component. Up to a 60-s plasma-polymerization time, the dipole–dipole forces provided by hydrogen bonding are stronger than the dispersion forces arising from van der Waals interactions on the PBZZ film surface formed by plasma-polymerization.

Surface Topographies

Figure 4 displays a series of SEM micrographs of BZZ films that we treated with various gas plasmas for different reaction times. The BZZ film surfaces after treatment with argon plasma have grid-like features [Fig. 4(a)]. The surface becomes rougher with longer reaction times and the features become smaller, more closely arranged, and more contorted.[25] Different features are observed in the oxygen plasma-treated BZZ films [Fig. 4(b)]. After plasma treatment for 30 s, the surface consists of evenly distributed nodules, each having a diameter of 20 nm. After the BZZ film had been treated for 60 s, the surface appears to have silk-like features in the gray section because the PBZZ polymer chains have formed around the nodules [Fig. 4(b)]. The diameters of

Figure 6. Effect of the argon, oxygen, and hydrogen plasma-polymerization with an increase of plasma treated time on the rms roughness of the PBZZ film at 1 μm × 1 μm image size.

these nodules decrease with increasing oxygen plasma treatment time, during which time the nodules become embedded in the PBZZ polymer chains. The hydrogen plasma treatment results in the porous features observed in Figure 4(c); the diameter of these pores increases with increasing plasma reaction time. Hydrogen atoms involved in a three-body collision process can form unstable molecules that are able to retain a greater portion of their recombination energy and may survive up to 10^8 collisions in the gas phase. Thus, chemical reactions by active hydrogen can arise from one or more of the following species: hydrogen atoms, excited hydrogen atoms, excited hydrogen molecules, protons, and other unstable complexes, such as H_x^*. These species cause the degradation of BZZ into alkane-like compounds that vaporize into the gas phase, which results in an etching effect. Therefore, we ascribed the observed morphologies to be the result of decomposition and polymerization reactions occurring simultaneously in the BZZ film during the hydrogen plasma-induced polymerization process.

Figure 5 provides a series of AFM images of PBZZ films that we had treated with argon, oxygen, and hydrogen plasmas for different periods of time; we performed these measurements on this series of samples to quantify the topographic changes. The AFM images of the surfaces of the BZZ films treated by argon plasma for different lengths of time [Fig. 5(a)] display a similar trend as that observed by SEM [Fig. 4(a)]. The vertical height of the features, measured from cross-sectional images, is of the order of 30 nm. The roughness of the argon plasma-treated surfaces increases with increasing reaction time and is similar, qualitatively, to that observed by SEM. Figure 5(b) displays images of the topographies of the BZZ films after oxygen plasma treatment for various periods of time. The number of surface nodules decreases as the reaction time increases and the vertical heights of the nodule structures, measured from cross-sectional images, are on the order of 5 nm.[26] This observation suggests that the polymerization of BZZ is initiated at the nodule structures. Figure 5(c) reveals AFM images of the BZZ films after they had been treated with hydrogen plasma for different periods of time. The vertical height of the surfaces in the cross-sectional images is on the order of 100 nm. The BZZ films treated with the hydrogen plasma clearly possess rougher surfaces as the reaction time increases that demonstrates the etching effect of the excited hydrogen atoms. Figure 6 illus-

trates the surface roughnesses, in image sizes of 1 μm $\times$ 1 μm, obtained after plasma treatment with the different carrier gases as a function of the reaction time. The surface roughness for the argon plasma-polymerization remains nearly constant with plasma-polymerization times of up to 90 s because the resistance toward the collision of argon atoms with high energy increases as PBZZ is formed. The roughness decreases with increasing oxygen plasma-polymerization time, which indicates that the sizes of the nodule structures decrease correspondingly. Decomposition and polymerization of BZZ occur simultaneously when using the excited hydrogen atom plasma and, thus, the roughness increases dramatically as the reaction time increases, resulting in the highest roughness observed among the three carrier gases used.

Etching Behavior

The BZZ films are polymerized by high-energy argon atoms, electronegative oxygen atoms, and excited hydrogen atoms, but these films are decomposed partially by the action of these atoms. High-energy atoms and ions present in these plasmas can react with the BZZ films to form volatile species, such as CO, CO_2, H_2O, and OH, to vaporize into the gas phase. Therefore, the CF_4 plasma resistance of the BZZ films is a very important property to ensure their etching reliabilities. Figure 7 presents estimates of the etching rates, based on changes in thickness after CF_4 plasma treatment, of the BZZ films prepared by treatment with the carrier gas plasmas. The oxygen plasma-polymerization provides the most stable PBZZ film, whereas both the hydrogen and argon plasma-polymerization processes result in simultaneous polymerization and decomposition of BZZ. The electronegative oxygen atoms induce BZZ polymerization without degradation, but the argon atoms and excited hydrogen atoms tend to break the alkyl bonds. Therefore, selecting a suitable carrier gas in which to conduct plasma-polymerization is an important factor to consider when polymerizing BZZ.

CONCLUSIONS

PBZZ thin films can be obtained by polymerizing BZZ with various plasmas as energy sources. The PBZZ films fabricated with plasmas of argon, oxygen, and hydrogen atoms possess grid-like, nod-

ular, and porous microstructures, respectively. The surface energy of the PBZZ film polymerized with oxygen plasma exhibits the highest hydrophilicity with respect to those prepared with the other carrier gases. The surface roughness of the PBZZ film depends on the type of carrier gas and the plasma-polymerization time. The hydrophilicity or hydrophobicity of the resulting PBZZ films can be controlled by selecting a suitable carrier gas during the plasma-polymerization process. The etching rate in CF_4 plasma, which we estimated by monitoring changes in thickness, indicates that the PBZZ film synthesized by oxygen plasma-polymerization possesses the highest plasma resistance.

REFERENCES AND NOTES

1. Gombotz, W. R.; Hoffman, A. S. Crit Rev Biocompatibility 1987, 4, 1.
2. Ratner, B. D.; Chilkoti, A.; Lopez, G. P. Plasma Deposition and Treatment for biomaterial applications. In Plasma Deposition, Treatment and Etching of Polymers. D'Agustino, R., Ed., Academic Press: New York, 1990, pp 463–516.
3. Kiaei, D.; Hoffman, A. S.; Horbett, T. A. J Biomater Sci Polym Ed 1992, 4, 35.
4. Lin, J. C.; Cooper, S. L. Biomaterials 1995, 16, 1017.
5. Lopez, G. P.; Ratner, B. D. Plasma Polym 1996, 1, 127.
6. Mahlberg, R.; Niemi, H. E.-M.; Denes, F. S.; Rowell, R. M. Langmuir 1999, 15, 2985.
7. Xiao, D.; Zhang, H.; Wirth, M. Langmuir 2002, 28, 9971.
8. Groenewoud, L. M. H.; Terlingen, J. G. A.; Engbers, G. H. M.; Feijen, J. Langmuir 1999, 15, 5396.
9. Schmidt, R.; Zhao, T.; Green, J. B.; Dyer, D. J. Langmuir 2002, 18, 1281.
10. Jordan, R.; Ulman, A.; Kang, J. F.; Rafailovich, M. H.; Sokolov, J. J Am Chem Soc 1999, 121, 1016.
11. Cruz-Barba, E.; Manolache, S.; Denes, F. Langmuir 2002, 18, 9393.
12. Kim, K. S.; Lee, K. H.; Cho, K.; Park, C. E. J Membr Sci 2002, 199, 135.
13. Wrobel, A. M.; Walkiewicz-Pietrzykowska, A. Chem Mater 2003, 15, 1749.
14. Wang, M. J.; Chang, Y. I.; Poncin-Epaillard, F. Langmuir 2003, 19, 8325.
15. Ishida, H. J Appl Polym Sci 1995, 58, 1751.
16. Ishida, H.; Low, H. Y. Macromolecules 1997, 30, 1099.
17. Ning, X.; Ishida, H. J Polym Sci Part B: Polym Phys 1994, 32, 921.
18. Ning, X.; Ishida, H. J Polym Sci Part A: Polym Chem 1994, 32, 1121.
19. Wu, S. Polymer Interface and Adhesion; Chapman and Hall: London, 1987.
20. Tsibouklis, J.; Stone, M.; Thorpe, A. A.; Graham, P.; Nevell, T. G.; Ewen, R. J. Langmuir 1999, 15, 7076–7079.
21. Agag, T.; Takeichi, T. Macromolecules 2001, 34, 7257.
22. Ishid, H.; Sanders, D. P. Macromolecules 2000, 33, 8149.
23. Choi, D. M.; Park, C. K.; Cho, K.; Park, C. E. Polymer 1997, 38, 6243.
24. Kim, K. S.; Lee, K. H.; Cho, K.; Park, C. E. J Membr Sci 2002, 199, 135.
25. Youngblood, J. P.; McCarthy, T. J. Macromolecules 1999, 32, 6800.
26. Mahlberg, R.; Niemi, H. E. M.; Denes, F. S.; Rowell, R. M. Langmuir 1999, 15, 2985.